Heating and cooling of protons in the fast solar wind between 0.3 and 1 AU: Helios revisited

Petr Hellinger,[1,2] Lorenzo Matteini,[3] Štěpán Štverák,[1,2] Pavel M. Trávníček,[1,2,4] and Eckart Marsch[5]

[1] The proton thermal energetics in the fast solar wind between 0.3 and 1 AU is reinvestigated using the Helios 1 and 2 data. Closer to the Sun, it is estimated that, to account for the observed radial profiles of the proton parallel and perpendicular temperature, nonnegligible parallel cooling and perpendicular heating are necessary. Around 1 AU heating is needed in both directions. We also calculate the corresponding rates and find that in total significant interplanetary heating is necessary, in agreement with previous results. The possible influence that deceleration of fast solar wind streams due to interaction with slow ones has on the proton thermodynamics is evaluated.

Citation: Hellinger, P., L. Matteini, Š. Štverák, P. M. Trávníček, and E. Marsch (2011), Heating and cooling of protons in the fast solar wind between 0.3 and 1 AU: Helios revisited, *J. Geophys. Res.*, *116*, A09105, doi:10.1029/2011JA016674.

1. Introduction

[2] The thermodynamics of protons in the fast solar wind is far from being understood. Helios observations show that the total proton temperature falls off more slowly than what is expected from the adiabatic prediction (i.e., $T \propto R^{-4/3}$; for symbol definitions see Appendix A). This suggests a need for efficient proton heating. However, the protons in the fast solar wind are only weakly collisional and exhibit small heat fluxes [*Marsch*, 2011] so that one expects the double-adiabatic evolution (i.e., $T_\perp \propto B$, $T_\parallel \propto n^2/B^2$) [*Chew et al.*, 1956], which in general would lead to an evolution quite different from $T \propto R^{-4/3}$ [cf. *Matteini et al.*, 2011].

[3] However, solar wind protons do not follow the double adiabatic prediction; their perpendicular temperature decreases with distance more slowly, whereas the parallel temperature decreases faster than what is expected from the double-adiabatic prediction [*Marsch et al.*, 1982b]. These observed departures from the double-adiabatic behavior clearly indicate a need of efficient perpendicular heating and parallel cooling of protons (and/or energy exchange between the two directions [cf. *Marsch and Richter*, 1987]).

[4] To determine mechanisms which could possibly be responsible for these proton thermal properties, it is important to quantify the necessary heating rates. *Vasquez et al.* [2007] and *Cranmer et al.* [2009] and others have used isotropic fluid equation to estimate the heating rates. However, as the pro-

tons in the fast solar wind are essentially collisionless and exhibit clear temperature anisotropies [*Hellinger et al.*, 2006; *Marsch et al.*, 2006; *Matteini et al.*, 2007] and heat fluxes owing a to presence secondary/beam populations, it is necessary to investigate the parallel and perpendicular temperatures separately [*Marsch et al.*, 1983; *Marsch and Richter*, 1987]. To estimate the particle heating rates a constant radial velocity component of the solar wind is typically assumed. However, continuous interactions between slow and fast streams are ubiquitous near the ecliptic plane, inducing variations in the solar wind bulk velocity (deceleration of fast streams and acceleration of slow ones), and consequently affecting the proton energetics. In this paper we estimate the parallel and perpendicular heating/cooling rates in the fast solar wind in the inner heliosphere, using in situ Helios 1 and 2 data. We assume a constant radial velocity as well as a decelerating solar wind.

[5] This paper is organized as follows. Theoretical predictions are given in section 2, the Helios data are analyzed in section 3 where the radial profiles of the proton moments are estimated, and resulting heating rates are derived. The obtained results are summarized and discussed in section 4.

2. Theoretical Predictions

[6] Taking moments of the Boltzmann equation one can derive the following fluid equations for the evolution of the parallel and perpendicular proton temperatures [cf. *Barakat and Schunk*, 1982; *Marsch et al.*, 1983]:

$$nk_B\left(\frac{\partial}{\partial t} + \boldsymbol{u} \cdot \boldsymbol{\nabla}\right)T_\parallel = nk_B\left[-2T_\parallel \boldsymbol{\nabla}_\parallel \cdot \boldsymbol{u} + \left(\frac{\mathrm{d}T_\parallel}{\mathrm{d}t}\right)_c\right]$$
$$- \boldsymbol{\nabla} \cdot (q_\parallel \boldsymbol{b}) + 2q_\perp \boldsymbol{\nabla} \cdot \boldsymbol{b},$$

$$nk_B\left(\frac{\partial}{\partial t} + \boldsymbol{u} \cdot \boldsymbol{\nabla}\right)T_\perp = nk_B\left[-T_\perp \boldsymbol{\nabla}_\perp \cdot \boldsymbol{u} + \left(\frac{\mathrm{d}T_\perp}{\mathrm{d}t}\right)_c\right]$$
$$- \boldsymbol{\nabla} \cdot (q_\perp \boldsymbol{b}) - q_\perp \boldsymbol{\nabla} \cdot \boldsymbol{b}, \qquad (1)$$

[1]Astronomical Institute, AS CR, Prague, Czech Republic.
[2]Institute of Atmospheric Physics, AS CR, Prague, Czech Republic.
[3]Dipartimento di Fisica e Astronomia, Università degli Studi di Firenze, Florence, Italy.
[4]SSL, University of Berkeley, Berkeley, California, USA.
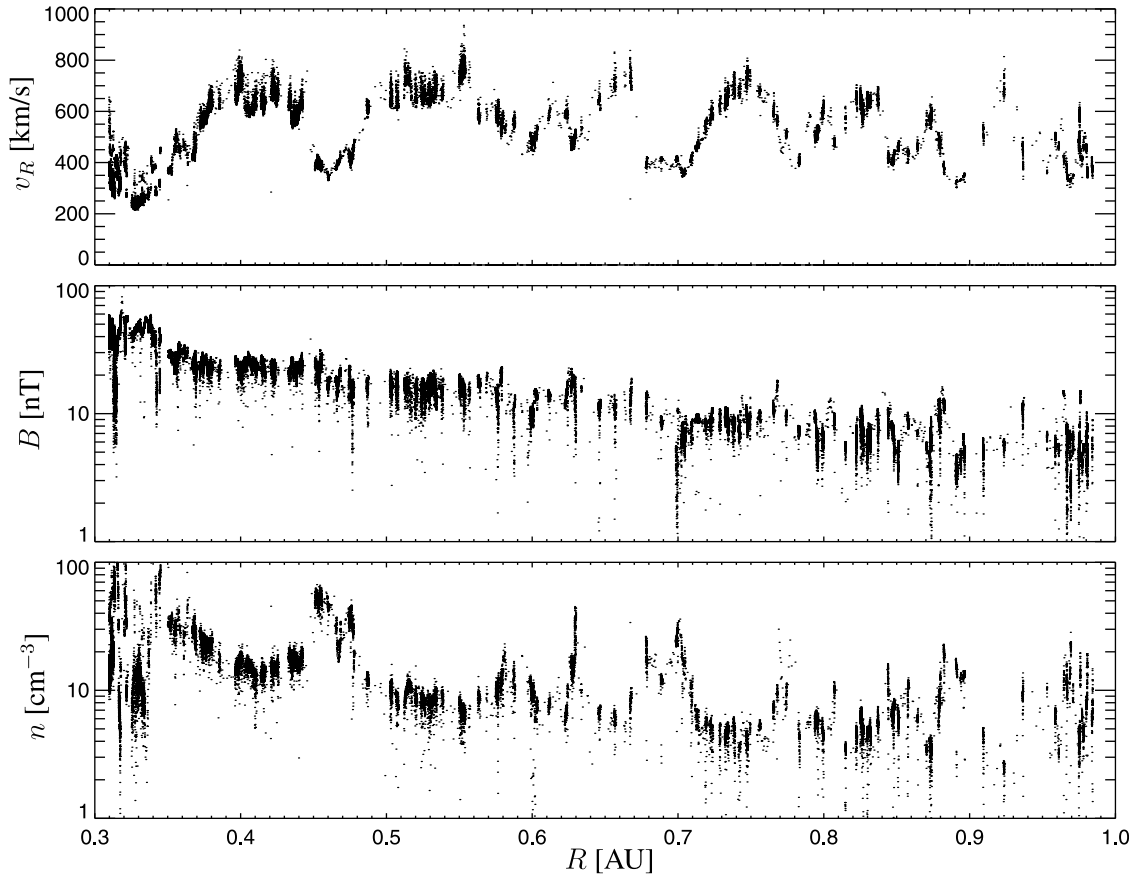[5]Max Planck Institut für Sonnensystemforschung, Katlenburg-Lindau, Germany.

Figure 1. Helios 1: Points show (top) proton radial velocity v_R, (middle) magnitude of the magnetic field B, and (bottom) proton density n as a function of the radial distance R during a part of the spacecraft trajectory (from January to March in 1976).

where $\nabla_\parallel = \boldsymbol{b}\,(\boldsymbol{b} \cdot \nabla)$ and $\nabla_\perp = \nabla - \nabla_\parallel$; note that all other symbols are defined in Appendix A. The collision terms in equation (1) are assumed to have the simple form:

$$\left(\frac{dT_\perp}{dt}\right)_c = -\frac{1}{2}\left(\frac{dT_\parallel}{dt}\right)_c = -\nu_T\left(T_\perp - T_\parallel\right), \qquad (2)$$

where the isotropization frequency ν_T may be calculated for a bi-Maxwellian velocity distribution function and expressed in terms of the Gauss hypergeometric function [*Kogan*, 1961; *Hellinger and Trávníček*, 2009]. When no collision and no heat fluxes are present the anisotropic equation (1) predicts the double-adiabatic evolution

$$T_\perp \propto B \quad \text{and} \quad T_\parallel \propto \frac{n^2}{B^2}. \qquad (3)$$

For completeness, in the isotropic case one recovers

$$n k_B\left(\frac{\partial}{\partial t} + \boldsymbol{u} \cdot \nabla\right)T = -\frac{2}{3}n k_B T \nabla \cdot \boldsymbol{u} - \nabla \cdot (q\boldsymbol{b}). \qquad (4)$$

3. Helios Observations

3.1. Solar Wind Variations

[7] Here we use data from ion analyzers and fluxgate magnetometers onboard the Helios 1 and 2 spacecraft

[*Marsch et al.*, 1982a, 1982b, and references therein]. The Helios analyzers employ a quadrispherical ion electrostatic deflector that analyzes ions with respect to their charge-per-energy ratio. A full three-dimensional spectrum, 32 channels (exponentially distributed between 155 V and 15.3 kV) times 9 × 16 angular channels (with the resolution 5° × 5° making use of the spacecraft rotation) is measured every 40.5 s. In this paper we use these 3-D energy spectra to calculate the basic moments of the proton velocity distribution function; the contribution of alpha particles is removed by using their different charge-to-mass ratio [*Marsch et al.*, 1982b]. We calculate the proton number density, n, radial component of the mean velocity, v_R, parallel and perpendicular temperatures, $T_\parallel$ and $T_\perp$, and both non-zero components of the heat flux tensor, $q_\parallel$ and $q_\perp$. Note that the temperatures and heat fluxes are calculated for the whole observed proton distribution functions. A possible secondary proton population contributes to the parallel temperature and to the heat fluxes.

[8] We start our data analysis with some typical radial profiles of observed solar wind quantities. Figure 1 displays the radial profiles of the proton radial velocity v_R, the magnitude of the magnetic field B, and the proton density n, as observed by Helios 1 from January to March in 1976. Only selected data are used, for which it is easily possible to separate the proton and alpha-particle contributions in the 3-D velocity spectra. Figure 1 illustrates some general
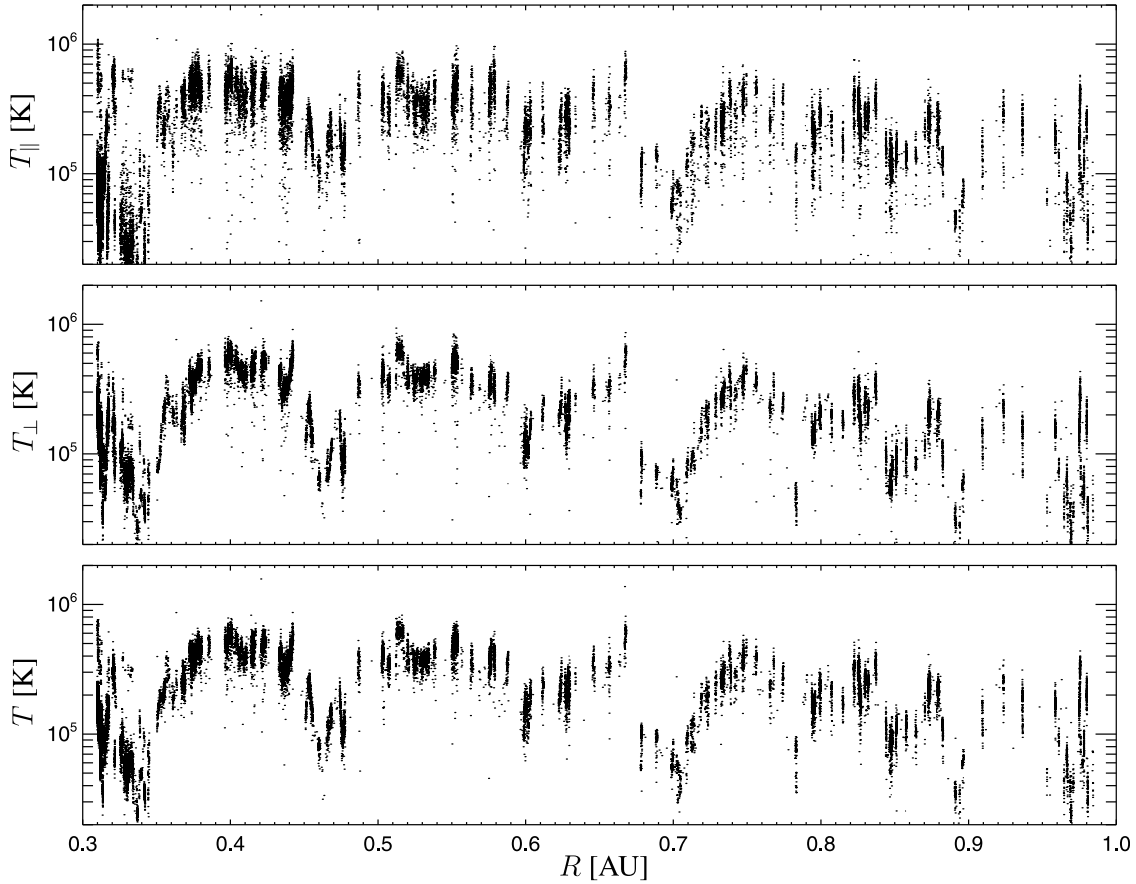
Figure 2. Helios 1: Points show (top) parallel proton temperature $T_\parallel$, (middle) perpendicular proton temperature $T_\perp$, and (bottom) average proton temperature T as a function of the radial distance R during a part of the spacecraft trajectory (from January to March in 1976, same as in Figure 1).

features of the solar wind in the ecliptic plane: the solar wind is characterized by alternating slow and fast streams. The magnitude of the magnetic field decreases with the radial distance R. The proton density and the radial velocity exhibit a well known anti-correlation.

[9] Figure 2, laid out in the same format as Figure 1, shows the radial profiles of the parallel and perpendicular proton temperatures, $T_\parallel$ and $T_\perp$, as well as of the averaged proton temperature T observed by Helios 1 from January to March in 1976. Figure 2 illustrates the well known correlation between the proton temperature and the velocity [cf. *Elliott et al.*, 2010], which holds also for the parallel and perpendicular proton temperatures.

3.2. Radial Dependencies

[10] Following *Cranmer et al.* [2009] we try to determine the radial dependence of the parallel and perpendicular temperatures in the fast solar wind, in order to estimate the energy balance of the protons. We use the whole data set of 3-D ion energy spectra from both Helios spacecrafts, but select only those data where it was easy to separate alpha-particles from protons. Here we only investigate the fast solar wind. Therefore, we have selected only those cases in which the proton radial velocity $v_R > 600$ km/s.

[11] These data are shown in Figure 3 where points represent the observed proton radial velocity v_R (Figure 3, top), magnitude of the magnetic field B (Figure 3, middle), and

proton density n as a function of the radial distance R (Figure 3, bottom). Figure 3 (top) clearly reveals the arbitrary speed cut-off at 600 km/s. On this panel one can also discern at some places signatures of local maxima of v_R (see Figure 1).

[12] The radial dependence of the proton number density and the magnitude of the magnetic field could be fitted (using the least squares linear regression function $\log(n, b) = a\log R + b$)) as

$$B \simeq 5.8(R/R_0)^{-1.6} \text{ nT}$$

$$n \simeq 2.8(R/R_0)^{-1.8} \text{ cm}^{-3}$$

(5)

where $R_0 = 1$ AU. The solid curves on Figures 3 (middle) and 3 (bottom) show the fitted dependencies according to equation (5). A short comment is in order here. The fitted dependence for the proton density decreases more slowly than R^{-2}, which is expected for a stationary radially expanding solar wind. The slower than R^{-2} decrease could indicate a plasma compression due to deceleration. While this result may be related to uncertainties of the fitting method the deceleration may be real, owing to the physical interaction between fast and slow streams.

[13] Results for the proton temperatures calculated from the 3-D energy spectra are shown in Figure 4; here points represent combined Helios 1 and 2 observations, with par-
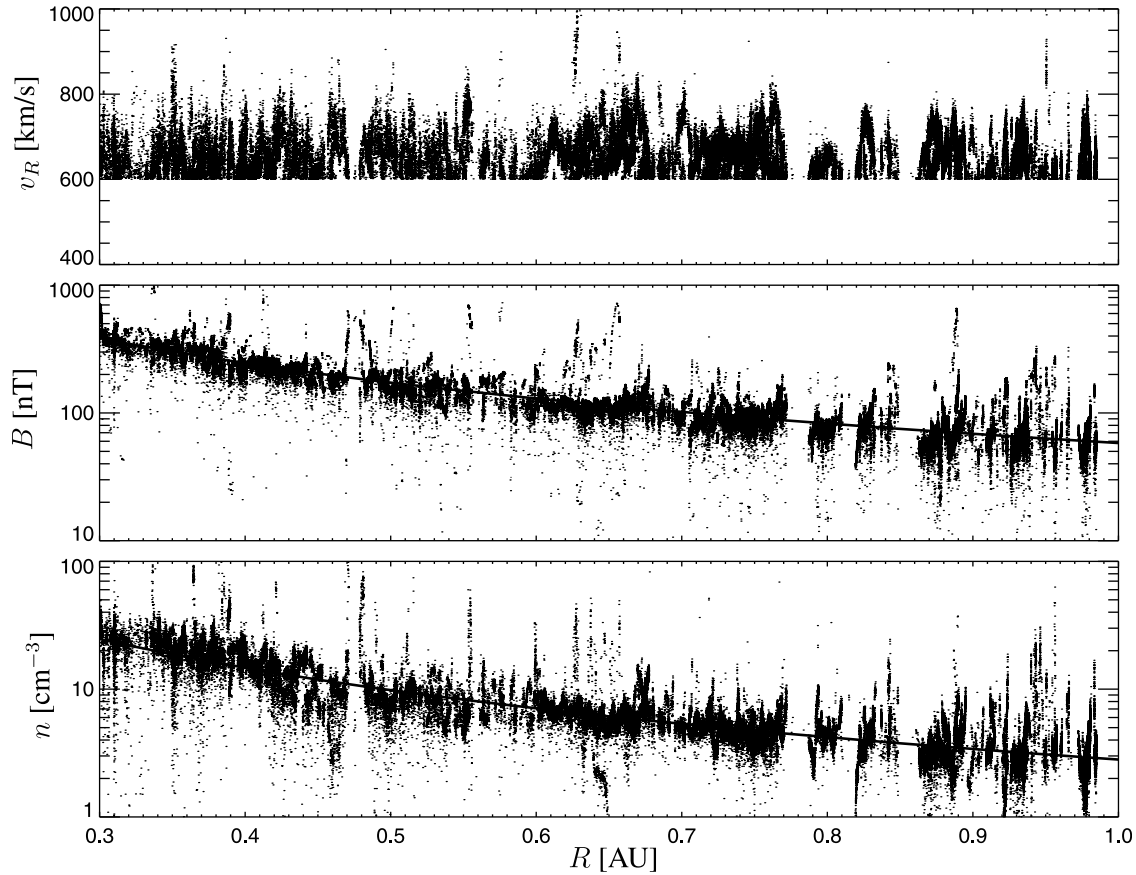
Figure 3. Helios 1 and 2 observations: Points show (top) proton radial velocity v_R, (middle) magnitude of the magnetic field B, and (bottom) proton density n as a function of the radial distance R. Overplotted solid curves show the fitted results (see the text).

allel proton temperature $T_\parallel$ (Figure 4, top), perpendicular proton temperature $T_\perp$ (Figure 4, middle), and average proton temperature T given as functions of the radial distance R (Figure 4, bottom). All the temperatures decrease with R. These dependencies may be approximated by the fits

$$T_\parallel \simeq 2.7 \cdot 10^5 (R/R_0)^{-0.54} \text{ K},$$

$$T_\perp \simeq 2.4 \cdot 10^5 (R/R_0)^{-0.83} \text{ K}, \qquad (6)$$

$$T \simeq 2.5 \cdot 10^5 (R/R_0)^{-0.74} \text{ K},$$

which are overplotted on Figure 4.

[14] Finally, we calculate heat fluxes from the 3-D energy spectra. Figure 5 shows points, obtained from the combined Helios 1 and 2 observations, denoting heat flux $q_\parallel$ (Figure 5, top), heat flux $q_\perp$ (Figure 5, middle), and average heat flux q (Figure 5, bottom) as functions of the radial distance R. Heat fluxes are given in units of W/m^2 = 1000 erg/s/cm^2. Overplotted solid curves show the fitted results

$$q_\parallel \simeq 4.8 \cdot 10^{-7} (R/R_0)^{-2.9} \text{ W/m}^2,$$

$$q_\perp \simeq 4.8 \cdot 10^{-8} (R/R_0)^{-2.8} \text{ W/m}^2, \qquad (7)$$

$$q \simeq 2.0 \cdot 10^{-7} (R/R_0)^{-2.8} \text{ W/m}^2.$$

All these derived radial profiles in the fast solar wind of the proton temperatures, equation (6), and the heat fluxes, equation (7), are close to the previous Helios results [*Marsch*, 1991]. It is important to note that the proton parallel heat flux $q_\parallel$ is comparable with the corresponding saturation heat flux $q_{\mathrm{sat}} = n \, (k_B \, T_\parallel)^{3/2}/m^{1/2}$ [cf. *Marsch et al.*, 1982b, Figure 17] indicating the presence of a nonnegligible secondary/beam population or a distorted proton velocity distribution function [*Feldman et al.*, 1973].

3.3. Heating Rates

[15] The fitted results from the previous section can be now used to test the proton thermal energetics expected from equation (1). Let us first investigate the two terms, $Q_\parallel$ and $Q_\perp$, given as

$$Q_\parallel = nk_{\mathrm{B}} \left(\boldsymbol{u} \cdot \nabla T_\parallel + 2T_\parallel \nabla_\parallel \cdot \boldsymbol{u} \right),$$

$$Q_\perp = nk_{\mathrm{B}} \left(\boldsymbol{u} \cdot \nabla T_\perp + T_\perp \nabla_\perp \cdot \boldsymbol{u} \right), \qquad (8)$$

where we have assumed a stationary solar wind proton velocity. The two terms include the collisional isotropization, heat fluxes and any necessary additional energy exchanges. For the calculation of $Q_\parallel$ and $Q_\perp$ we assume a
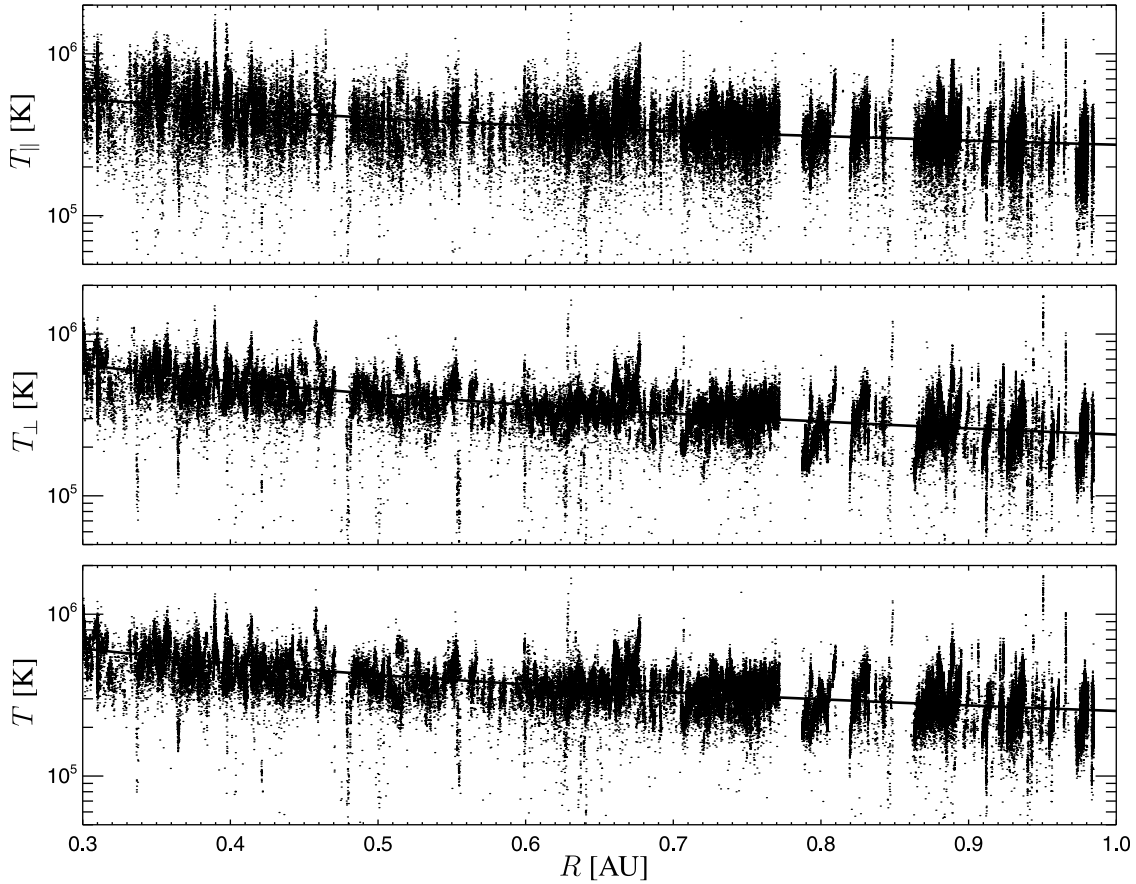
Figure 4. Helios 1 and 2 observations: Points show (top) parallel proton temperature $T_\parallel$, (middle) perpendicular proton temperature $T_\perp$, and (bottom) average proton temperature T as functions of the radial distance R. Overplotted solid curves show fitted results (see the text).

constant radial velocity $v_{sw} = 700$ km/s, and for the proton density we assume

$$n = 2.6(R/R_0)^{-2} \text{ cm}^{-3}, \tag{9}$$

to be compatible with a constant radial velocity. For the temperatures and heat fluxes we assume equations (6) and (7), and for the magnetic field we assume that it follows the Parker spiral (with the radial and transverse components of the magnetic field, $B_r \propto \cos\theta \ (R/R_0)^{-2}$ and $B_t \propto \sin\theta \ (R/R_0)^{-1}$, with $\theta = 45^\circ$). For these parameters it follows first that the collisional transport coefficients as well as the contribution of heat fluxes are negligible as expected, so that $Q_\parallel$ and $Q_\perp$ are the necessary heating/cooling rates. Figure 6 shows the result of the calculation, $Q_\parallel$, $Q_\perp$, and the average heating rate $Q = (Q_\parallel + 2Q_\perp)/3$.

[16] Figure 6 shows the estimated heating rates: absolute value of parallel heating rate $Q_\parallel$ (dotted line denotes negative values of $Q_\parallel$ whereas solid line denotes positive values) (Figure 6, top), perpendicular heating rate $Q_\perp$ (Figure 6, middle), and average heating rate Q (Figure 6, bottom) as functions of R. The volumetric heating rates are given in units of W/m^3 (= 10^{16} erg/s/cm^3). Figure 6 quantifies the well known results: the proton parallel temperature in the solar wind tends to decrease faster than what is expected

from the double-adiabatic prediction, whereas the perpendicular temperature decreases more slowly than expected. Consequently, a parallel cooling and perpendicular heating are necessary below ~0.6 AU. Yet above ~0.6 AU parallel heating is certainly needed. The parallel cooling and the perpendicular heating rates are of the same order. Thus some (anomalous) energy transfer mechanism from parallel to perpendicular direction may be at work here. For estimates of the involved transfer times, see *Marsch and Richter* [1987]. However, in total, the system needs to be heated with the net heating rate Q (Figure 6, bottom), which may be fitted as

$$Q \simeq 0.24 \cdot 10^{-16}(R/R_0)^{-3.8} \text{ W/m}^3. \tag{10}$$

It is interesting to note that from equation (4) one gets essentially the same result for the heating rate Q.

3.4. Influence of Deceleration

[17] In the previous section we have assumed a constant component of the radial proton velocity. The observations, however, indicate a slight deceleration of fast solar wind streams, and so it is interesting to estimate its influence on the proton energetics. A simple way how to do it is to
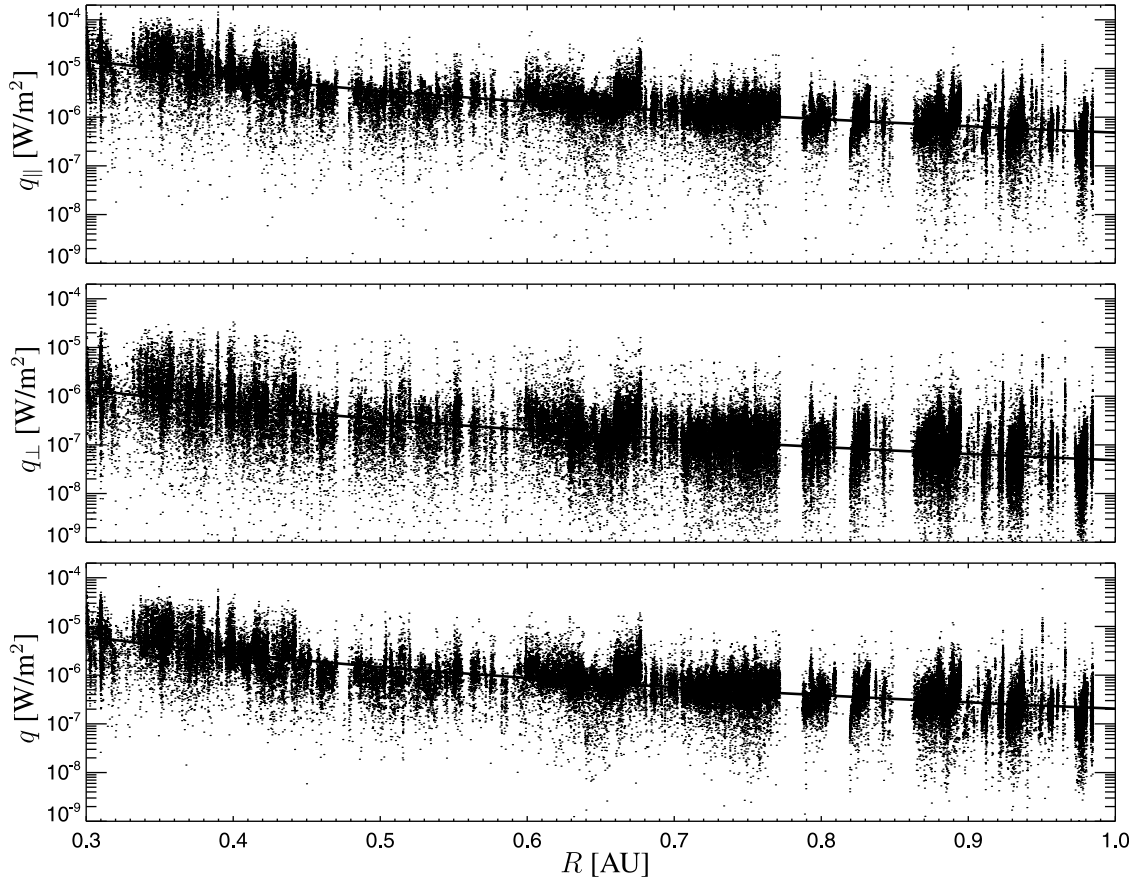
Figure 5. Helios 1 and 2 observations: Points show (top) heat flux $q_{\parallel}$, (middle) heat flux $q_{\perp}$, and (bottom) average heat flux q as functions of the radial distance R. Overplotted solid curves show fitted results (see the text).

assume a proton velocity compatible with the fitted density profile (equation (5)). If we take

$$v_{sw} = 600 \, (R/R_0)^{-0.19} \text{ km/s}, \tag{11}$$

then we can recalculate the heating rates from equation (8). Figure 7 displays parallel heating rate $Q_{\parallel}$ (Figure 7, top), perpendicular heating rate $Q_{\perp}$ (Figure 7, middle), and average heating rate Q (Figure 7, bottom) calculated for the velocity profile, equation (11). The dashed line displays the fitted result

$$Q \simeq 0.17 \cdot 10^{-16} (R/R_0)^{-3.9} \text{ W/m}^3. \tag{12}$$

Again, from the isotropic approximation, equation (4), one gets essentially the same result for the volumetric heating rate Q.

[18] In this analysis, where we assumed a decelerating solar wind, the necessary total heating rate dropped by about 30 %, in comparison to the constant speed approximation. Moreover, the necessary cooling rate in the parallel direction increased when compared with the constant velocity approximation, whereas the perpendicular heating rates are similar in the two cases, since only the parallel temperature depends on the density in the radial dependence of the double-adiabatic prediction given by equation (3).

4. Discussion

[19] In this paper we have estimated the heating and cooling rates for protons in the fast solar wind. The energy exchanges between the parallel and perpendicular directions due to Coulomb collisions are negligible. The proton distribution function exhibit an important heat flux (comparable to the saturation value) consistent with a presence of an important secondary/beam population. However, the contribution of the proton heat flux to the collisionless proton energy radial transfer is negligible. Assuming a constant velocity solar wind, the total heating rates estimated from both the anisotropic and isotropic temperature equations are essentially the same. The rates compare well with the previous ones based on the isotropic temperature approximation [*Vasquez et al.*, 2007; *Cranmer et al.*, 2009]. However, the anisotropic description is necessary, as the parallel and perpendicular temperatures evolve differently, and since the resulting amount of total heating is a combination of parallel cooling and perpendicular heating. Our results strongly suggest the presence of an efficient transfer of thermal energy from the parallel to the perpendicular direction
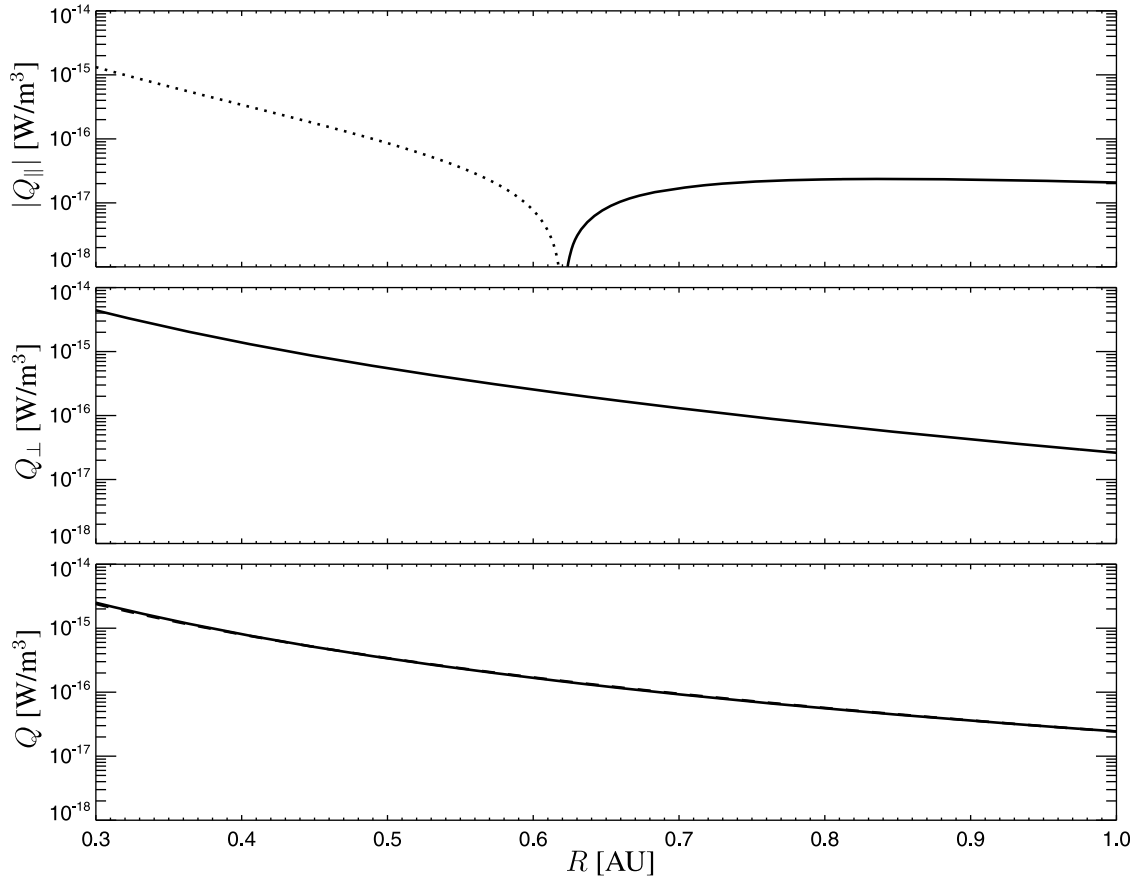
Figure 6. Estimated heating rates from the fitted data (assuming a constant solar wind velocity): (top) absolute value of the parallel heating rate $Q_\parallel$ (the dotted line denotes negative values of $Q_\parallel$, whereas the solid line denotes positive values), (middle) perpendicular heating rate $Q_\perp$, and (bottom) average heating rate Q. The dashed line displays a fitted result of $Q = Q(R)$, equation (10).

[Marsch and Richter, 1987]. It is important to fully understand this mechanism, its physical properties, and their role in the proton heating/cooling, in order to constrain the possible heating associated with other processes such as turbulent heating [Matteini et al., 2011]. This mechanism is possibly of kinetic nature and is likely related to observed deceleration of the secondary/beam population with respect to the core protons [Marsch et al., 1982b]. Such a deceleration naturally leads to the parallel cooling and may be partly responsible for the observed perpendicular heating [Schwartz et al., 1981].

[20] The present heating rates have been estimated by use of fitted radial profiles of the proton velocity moments calculated from the 3-D Helios ion spectra. However, there are large uncertainties of the measured quantities (especially for higher moments), and moreover, the solar wind in the ecliptic plane is characterized by alternating fast and slow streams. The Helios data indeed indicate that the proton density in the fast solar wind decreases more slowly than what is expected from a constant radial component of the solar wind velocity. This finding is compatible with deceleration of the fast streams as they interact with slow ones. A simple estimation of the heating and cooling rates in a stationary decelerating solar wind (compatible with the fitted density profile) gives an important reduction of the necessary total heating. While the required perpendicular heating is similar to that in the case of a constant solar wind velocity, the necessary parallel cooling (and/or energy transfer from parallel to perpendicular direction) then is significantly larger. We note however that the interaction between slow and fast streams is a complex phenomenon including compression and rarefraction regions [cf. Elliott et al., 2005] and requires a much more detailed study which is beyond the scope of this paper. Further investigation of the evolution of proton temperatures (or rather of the full proton velocity distribution function) is needed. It seems clear that one should, when studying the thermodynamics, try to measure the undisturbed solar wind streams at higher latitudes (or closer to Sun) in the inner heliosphere, because the interaction between streams is expected to be absent (or reduced) there.

Appendix A: Glossary

[21] Here $\boldsymbol{B}$ is the magnetic field, $B = |\boldsymbol{B}|$ being its amplitude; $\boldsymbol{b}$ is the unit vector along the magnetic field, $\boldsymbol{b} = \boldsymbol{B}/B$; R stands for the radial distance from the Sun. Here f denotes the proton velocity distribution function which is assumed to be gyrotropic. Subscripts $\perp$ and $\parallel$ denote the directions with respect to the ambient magnetic
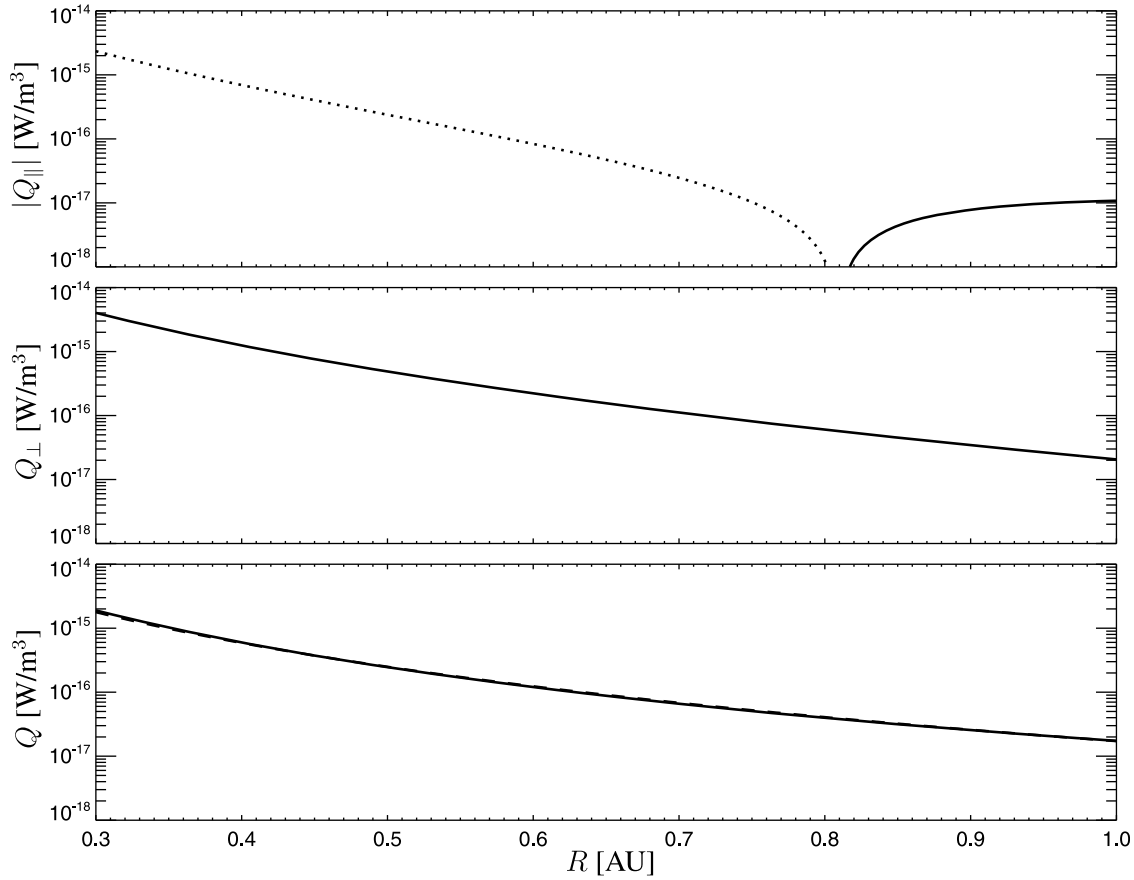
Figure 7. Estimated heating rates from the fitted data (assuming a decelerating solar wind, equation (11)): (top) absolute value of the parallel heating rate $Q_\parallel$ (Dotted line denotes negative values of $Q_\parallel$, whereas solid line denotes positive values.), (middle) perpendicular heating rate $Q_\perp$, and (bottom) average heating rate Q. The dashed line displays the fitted result, equation (12).

field. n is the proton density $n = \int f \mathrm{d}^3 v$, $\boldsymbol{u}$ is the mean velocity $\boldsymbol{u} = \int \boldsymbol{v} f \mathrm{d}^3 v$. The parallel and perpendicular proton temperatures are given as $T_\parallel = (m/k_B\, n) \int v_\parallel^2 f \mathrm{d}^3 v$ and $T_\perp = (m/2k_B\, n) \int v_\perp^2 f \mathrm{d}^3 v$, respectively, where $v_\parallel = \boldsymbol{b} \cdot (\boldsymbol{v} - \boldsymbol{u})$, $v_\perp^2 = |(\boldsymbol{v} - \boldsymbol{u})|^2 - v_\parallel^2$, m is the proton mass, k_B is the Boltzmann constant; $T = (2T_\perp + T_\parallel)/3$ is the total proton temperature. The two nonzero components of the heat flux tensor are given as $q_\parallel = m \int v_\parallel^3 f \mathrm{d}^3 v$ and $q_\perp = (m/2) \int v_\parallel v_\perp^2 f \mathrm{d}^3 v$; $q = (2q_\perp + q_\parallel)/3$ being the total proton heat flux. Here, $Q_\perp$ and $Q_\parallel$, are the necessary perpendicular and parallel heating rates, $Q = (2Q_\perp + Q_\parallel)/3$ being the averaged heating rate.

References

Barakat, A. R., and R. W. Schunk (1982), Transport equations for multi-component anisotropic space plasmas: A review, *Plasma Phys.*, *24*, 389–418.

Chew, G. F., M. L. Goldberger, and F. E. Low (1956), The Boltzmann equation and the one fluid hydromagnetic equations in the absence of particle collisions, *Proc. R. Soc. London, Ser. A*, *236*, 112–118.

Cranmer, S. R., W. H. Matthaeus, B. A. Breech, and J. C. Kasper (2009), Empirical constraints on proton and electron heating in the fast solar wind, *Astrophys. J.*, *702*, 1604–1614.

Elliott, H. A., D. J. McComas, N. A. Schwadron, J. T. Gosling, R. M. Skoug, G. Gloeckler, and T. H. Zurbuchen (2005), An improved expected temperature formula for identifying interplanetary coronal mass ejections, *J. Geophys. Res.*, *110*, A04103, doi:10.1029/2004JA010794.

Elliott, H. A., D. J. McComas, W. H. Matthaeus, and C. J. Henney (2010), Solar wind speed and temperature relationship, in *Twelfth International Solar Wind Conference*, edited by M. Maksimovic et al., *AIP Conf. Proc.*, *1216*, 98–101.

Feldman, W. C., J. R. Asbridge, S. J. Bame, and M. D. Montgomery (1973), On the origin of solar wind proton thermal anisotropy, *J. Geophys. Res.*, *78*, 6451–6468.

Hellinger, P., and P. M. Trávníček (2009), On Coulomb collisions in bi-Maxwellian plasmas, *Phys. Plasmas*, *16*, 054501.

Hellinger, P., P. Trávníček, J. C. Kasper, and A. J. Lazarus (2006), Solar wind proton temperature anisotropy: Linear theory and WIND/SWE observations, *Geophys. Res. Lett.*, *33*, L09101, doi:10.1029/2006GL025925.

Kogan, V. I. (1961), The rate of equalization of the temperatures of charged particles in a plasma, in *Plasma Physics and the Problem of Controlled Thermonuclear Reactions*, vol. 1, edited by M. A. Leontovich, pp. 153–161, Pergamon, New York.

Marsch, E. (1991), Kinetic physics of the solar wind plasma, in *Physics of the Inner Heliosphere II. Particles, Waves and Turbulence*, *Phys. Chem. Space Space Sol. Phys.*, vol. 21, edited by R. Schwenn and E. Marsch, pp. 45–110, Springer-Verlag, Berlin.

Marsch, E. (2011), Helios: Evolution of distribution functions 0.3–1 AU, *Space Sci. Rev.*, doi:10.1007/s11214-010-9734-z, in press.

Marsch, E., and A. K. Richter (1987), On the equation of state and collision time for a multicomponent, anisotropic solar wind, *Ann. Geophys.*, *5A*, 71–82.

Marsch, E., K. H. Mühlhäuser, H. Rosenbauer, R. Schwenn, and F. M. Neubauer (1982a), Solar wind helium ions: Observations of the Helios solar probes between 0.3 AU and 1 AU, *J. Geophys. Res.*, *87*, 35–51.

Marsch, E., K. H. Mühlhauser, R. Schwenn, H. Rosenbauer, W. Pilipp, and F. M. Neubauer (1982b), Solar wind protons: Three-dimensional velocity distributions and derived plasma parameters measured between 0.3 AU and 1 AU, *J. Geophys. Res.*, *87*, 52–72.

Marsch, E., K. H. Mühlhäuser, H. Rosenbauer, and R. Schwenn (1983), On the equation of state of solar wind ions derived from helios measurements, *J. Geophys. Res.*, *88*, 2982–2992.

Marsch, E., L. Zhao, and C.-Y. Tu (2006), Limits on the core temperature anisotropy of solar wind protons, *Ann. Geophys.*, *24*, 2057–2063.

Matteini, L., S. Landi, P. Hellinger, F. Pantellini, M. Maksimovic, M. Velli, B. E. Goldstein, and E. Marsch (2007), The evolution of the solar wind proton temperature anisotropy from 0.3 to 2 AU, *Geophys. Res. Lett.*, *34*, L20105, doi:10.1029/2007GL030920.

Matteini, L., P. Hellinger, S. Landi, P. M. Travnicek, and M. Velli (2011), Ion kinetics in the solar wind: Coupling global expansion to local microphysics, *Space Sci. Rev.*, doi:10.1007/s11214-011-9774-z, in press.

Schwartz, S. J., W. C. Feldman, and S. P. Gary (1981), The source of proton anisotropy in the high-speed solar wind, *J. Geophys. Res.*, *86*, 541–546.

Vasquez, B. J., C. W. Smith, K. Hamilton, B. T. MacBride, and R. J. Leamon (2007), Evaluation of the turbulent energy cascade rates from the upper inertial range in the solar wind at 1 AU, *J. Geophys. Res.*, *112*, A07101, doi:10.1029/2007JA012305.

P. Hellinger, Š. Štverák, and P. M. Trávníček, Astronomical Institute, AS CR, Bocni II/1401, Prague 14131, Czech Republic. (petr.hellinger@ig.cas.cz; stverak@ig.cas.cz; trav@ig.cas.cz)

E. Marsch, Max Planck Institut für Sonnensystemforschung, Max Planck Strasse 2, D-37191 Katlenburg-Lindau, Germany. (marsch@linmpi.mpg.de)

L. Matteini, Dipartimento di Fisica e Astronomia, Università degli Studi di Firenze, Largo E. Fermi 2, I-50125 Firenze, Italy. (matteini@arcetri.astro.it)